

Large-Scale Structure from Galaxy and Cluster Surveys

Luigi Guzzo

INAF - Osservatorio Astronomico di Brera, Via Bianchi 46, I-23807 Merate (LC), Italy

Abstract. I review the status of large-scale structure studies based on redshift surveys of galaxies and clusters of galaxies. In particular, I compare recent results on the power spectrum and two-point correlation correlation function from the 2dF and REFLEX surveys, highlighting the advantage of X-ray clusters in the comparison to cosmological models, given their easy-to-understand mass selection function. Unlike for galaxies, this allows the overall normalization of the power spectrum to be measured directly from the data, providing an extra constraint on the models. In the context of CDM models, both the shape and amplitude of the REFLEX $P(k)$ require, consistently, a low value for the mean matter density Ω_M . This shape is virtually indistinguishable from that of the galaxy power spectrum measured by the 2dF survey, simply multiplied by a constant cluster-galaxy bias factor. This consistency is remarkable for data sets which use different tracers and are very different in terms of selection function and observational biases. Similarly, the knowledge of the power spectrum normalization yields naturally a value $b \simeq 1$ for the bias parameter of b_J -selected (as in 2dF) galaxies, also in agreement with independent estimates using higher-order clustering and CMB data. In the final part, I briefly describe the measurements of the matter density parameter from redshift space distortions in galaxy surveys, and show evidence for similar streaming motions of clusters in the REFLEX redshift-space correlation function $\xi(r_p, \pi)$. With no exception, this wealth of independent clustering measurements point in a remarkably consistent way towards a low-density CDM Universe with $\Omega_M \simeq 0.3$.

1 Introduction

The last couple of years have witnessed an impressive series of achievements in the field of large-scale structure, thanks to ¹ new large surveys of galaxies and clusters of galaxies. The enthusiasm for new results on the clustering of galaxies and clusters has been strengthened by the unprecedented possibility to couple these to the anisotropies in the cosmic microwave background over an overlapping range of scales (see contributions by Melchiorri and Cooray, this volume).

In this brief review I have tried and provide a general guide for the non-specialist through some of the large-scale structure results. Clearly, such a review is far from being complete, although the references indicated should allow the

¹ Review to appear in *DARK2002, 4th Heidelberg Int. Conf. on Dark Matter in Astro- and Particle Physics*, (Cape Town, February 2002), H.-V. Klapdor-Kleingrothaus & R. Viollier eds., Springer

reader to find further links to the available literature on the subject (before February 2002). I therefore apologize to those colleagues whose work has not been adequately covered.

2 Cosmological Background

The currently popular model for the origin and evolution of structure in the expanding Universe is the Cold Dark Matter (CDM) model [1], whose global features provide a framework which is remarkably consistent with a large number of observations. The “Cosmology 2000” version of the model (often referred to in the recent literature as the ‘concordance’ model), which takes into account the independent evidences for a flat geometry (from the angular power spectrum of anisotropies in the Cosmic Microwave Background [2]) and an accelerated expansion (from the luminosity-distance relation of distant supernovae, used as “standard candles” [3]) is one where CDM, in the form of some kind of weakly-interacting non-relativistic particles (see pertinent articles in this volume), contributes about 25-30% of the total density, with the remaining 70% provided by a “dark energy” associated to a *Cosmological Constant*. I will comment at the end of this review on how comfortable we should feel in front of the number of “unseen” ingredients of this model. Here we shall use the model as it is, in fact “just a model”, i.e. a physically motivated machinery which works remarkably well when confronted with a variety of observations.

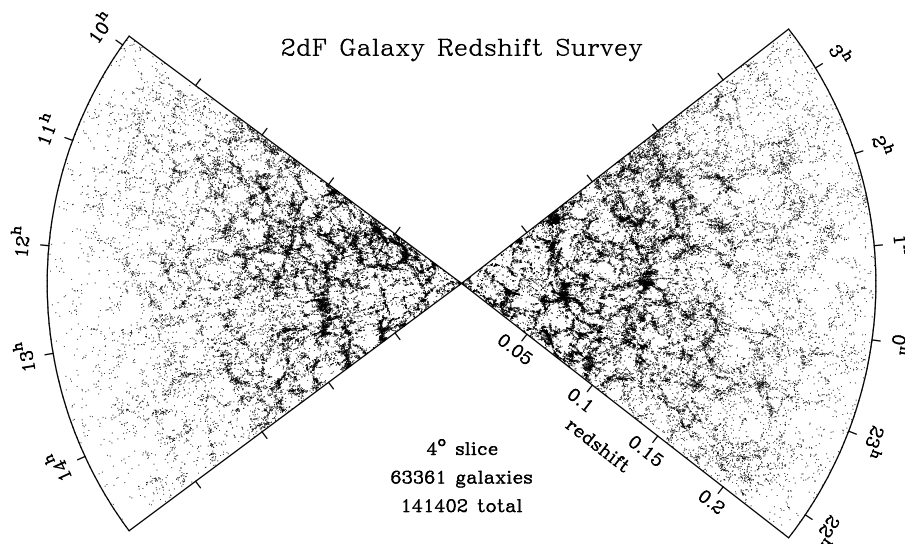


Fig. 1. The distribution of over 63,000 galaxies in two 4-degree thick slices extracted from the total of more than 210,000 galaxies that currently make up the 2dF Galaxy Redshift Survey (2dFGRS, figure from [14]).

Choosing CDM (or any other model) means specifying a *Transfer Function* $T(k)$. This can be thought of as describing a linear amplifier² which filters the primordial spectrum of fluctuations (typically of the scale-invariant form $P_o(k) \propto k$ generally predicted by inflation) to produce the shape of power spectrum we can still observe today on large [$k \lesssim 2\pi/(10 h^{-1} \text{ Mpc})$] scales, $P(k) = |T(k)|^2 P_o(k)$ [4,5]. One of the nice features of the CDM spectral shape in any of its variants is to naturally lead to a *hierarchical* growth of structures, where larger entities are continuously formed from the assembly of smaller ones [6]. Within the *gravitational instability* picture, the formation of galaxies and larger structures is completely driven by the gravitational field of the dark matter, with our familiar *baryonic* matter representing only a tiny bit of the mass (2 – 4% of the total energy density). The lighting-up of galaxies and other luminous objects depends then on how the baryons cool within the dark matter haloes and form stars, ending up as the only directly visible peaks of a much larger, invisible structure.

This increasing complexity in the physics involved in this cascade of processes is reflected by the limits in the predicting power of current detailed models of galaxy formation. Predictions from purely gravitational n-body experiments concerning the overall clustering of the dark mass can be regarded as fairly robust [7]. More complex semi-analytical calculations addressing the history of galaxy formation have seen exciting progress during the last few years [8,9,10,11], but they clearly still depend on a large number of not fully constrained parameters.

Direct measurements of large-scale structure are a classical test-bench for CDM models and they have, for example, been the reason for rejecting the original Einstein-DeSitter ($\Omega_{\text{Matter}} = 1$) version of the model, whose transfer function is inconsistent with the observed balance of large- to small-scale power [12]. The main problem in the game is that true direct measurements of mass structure (as e.g. through peculiar velocities or gravitational lensing cosmic shear), are not trivial: most observations have necessarily to use radiating objects as tracers of the mass distribution, and thus need to go through the uncertainties mentioned above to allow meaningful comparison to model predictions [13].

3 Progress in Large-Scale Structure Observations

3.1 Galaxy Redshift Surveys

Since the 1970's, redshift surveys of galaxies have represented the primary way to reconstruct the 3D topology of the Universe [15]. Year 2000 has seen the completion and public release [16] of the first 100,000 galaxy redshift measurements by the Anglo-Australian 2dF Galaxy Redshift Survey³, the largest complete sample of galaxies with measured distances to date [16,20]. This survey

² k is the Fourier wavenumber, i.e. the inverse of a 3D spatial scale $\lambda = 2\pi/k$, measured in $h^{-1} \text{ Mpc}$, with h being the Hubble constant in units of $100 h^{-1} \text{ Mpc}$. Most recent determinations indicate $h \simeq 0.7$ with about 10% error, see W. Freedman contribution to this volume.

³ <http://www.mso.anu.edu.au/2dFGRS>

includes all galaxies with blue magnitude b_J brighter than ~ 19.5 , mainly over two areas covering ~ 2000 square degrees in total, to an effective depth of about $600 h^{-1} \text{ Mpc}$ ($z \sim 0.2$). Its immediate precursors [17,18] reached a similar depth, but over much smaller areas: for comparison, the Las Campanas Redshift Survey (LCRS [17]), measured a total of 16,000 redshifts, against the 250,000 that will eventually form the full 2dF survey. A plot of the galaxy distribution within the two main sky regions of this survey is shown in Fig.1. Here one can appreciate in detail the wealth of structures typical of the distribution of galaxies: clusters, superclusters (filamentary or perhaps sheet-like) and *voids*, i.e. regions of very low galaxy density [15]. I will discuss the main clustering results from this survey in the following sections.

In a parallel effort, the Sloan Digital Sky Survey (SDSS)⁴ is covering a large fraction of the Northern sky with a uniform five-band CCD survey (u' , g' , r' , i' , z'), plus measuring redshifts for one million galaxies over the same area [21]. The photometry reaches a red magnitude $r' \sim 23$; the redshift survey is limited to galaxies brighter than $r' = 17.7$, resulting in a depth similar to that of ESP, LCRS and 2dF, but over a very large area. Early data over 462 square degrees have been recently released⁵. The SDSS represents the largest and most comprehensive galaxy survey work ever conceived: in addition to the redshift survey, the multi-band photometry is going to be of immense value for a number of studies, as estimating *photometric redshifts* [22,23] to much larger depth, or selecting samples with well-defined colour/morphology properties. A relevant example of such applications has been the discovery of several high-redshift ($z > 5$) quasars, including the $z = 6.28$ case for which the first possible detection of the long-sought Gunn-Peterson effect, essentially the fingerprint of the “dark-ages”, has been recently reported [24]. Another important application will be the selection of about 10^5 “red luminous” galaxies with $r' < 19.5$, that will be observed spectroscopically providing a nearly volume-limited homogeneous sample out to $z \simeq 0.5$, to study the clustering power spectrum on extremely large scales [25].

Both the 2dF and SDSS redshift surveys rely upon the large multiplexing performances of fiber-fed spectrographs, that allow the light from several hundred galaxies over a field of view of 1-2 degrees to be conveyed into the same slit on the spectrograph. This specific technology, in various forms, has been the key to the explosion of the redshift survey industry in the 1990’s, bringing the efficiency from the 10 redshifts/night for galaxies brighter than blue magnitude $b \sim 14$ of the 1970’s, to the current 2500 redshifts/night to $b \sim 19.5$ (see e.g. [26] for a more accurate account).

3.2 Surveys of X-ray Clusters of Galaxies

Clusters of galaxies are complementary tracers of large-scale structure (see e.g. [27]). Especially before the current era, when $N > 100,000$ galaxy redshifts are

⁴ <http://www.sdss.org/>

⁵ <http://archive.stsci.edu/sdss/>

becoming available over comparable volumes, groups and clusters have represented the most efficient alternative to map very large volumes of the Universe, exploring in this way the gross structure and its statistical properties in the weak clustering regime.

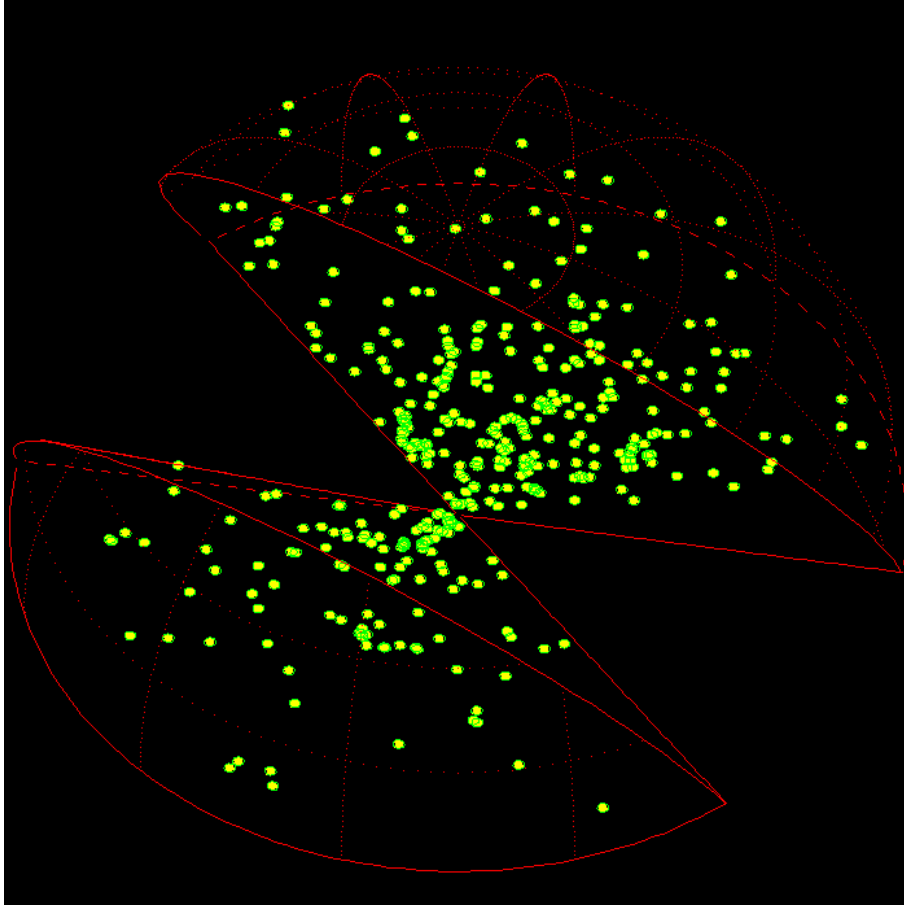


Fig. 2. The spatial distribution of X-ray clusters in the REFLEX survey, out to $600 h^{-1} \text{ Mpc}$ (from [13]). Note that here each point corresponds to a cluster, containing hundreds or thousands of galaxies. Structure is here mapped in a coarse way, yet sufficient to evidence very large structures as the “chains” of clusters visible in this picture.

X-ray selection represents currently the most physical way to identify large homogeneous samples of clusters of galaxies⁶ (see also discussion in [29]). Clusters shine in the X-ray sky due to the *bremsstrahlung* emission produced by a hot

⁶ A notable powerful alternative, so far limited by technical development, is represented by radio surveys using the Sunyaev-Zel’dovic effect. In this case one measures,

plasma ($kT \sim 1 - 10$ KeV) trapped within their potential wells. The bolometric emissivity (i.e. the energy released per unit time and volume) of this thin gas is proportional to its density squared and to $T^{1/2}$. Such dependence on n^2 makes clusters stand out more in the X-rays than in the optical light distribution ($\propto n$).

Under the assumption of hydrostatic equilibrium, the intracluster gas temperature, measured through the X-ray spectrum, is a direct probe of the cluster mass: $kT \propto \mu m_p \sigma_v^2 \sim G \mu m_p M_{vir} / (3r)$ (where m_p is the proton mass, $\mu \simeq 0.6$ the gas mean molecular weight, σ_v the galaxy 1D velocity dispersion and M_{vir} the cluster virial mass). X-ray luminosity, a more directly observable quantity with current instrumentation, shows a good correlation with temperature, $L_X \propto T^\alpha$ with $\alpha \simeq 3$ and a scatter $\lesssim 30\%$. The practical implication, even only on a phenomenological basis, is that clusters selected by X-ray luminosity are in practice mass-selected, with an error $\lesssim 35\%$ (see e.g. [30] and references therein for a more critical discussion). Last, but not least, the selection function of an X-ray cluster survey can be determined to high accuracy, knowing the properties of the X-ray telescope used, in a similar way to what is usually done with magnitude-limited samples of galaxies [31]. This is of fundamental importance if one wants to compute statistical quantities and test cosmological predictions as, e.g., the mean density or the clustering of clusters above a given mass threshold [13].

Fig. 2 plots the large-scale distribution of X-ray clusters from the REFLEX (ROSAT-ESO Flux Limited X-ray) cluster survey, the largest redshift survey of X-ray clusters with homogeneous selection function to date [32]. This data set, completed in 2000 and publicly released at the beginning of 2002, is based on the X-ray all-sky survey performed by the ROSAT satellite in the early 1990's (see e.g. [33,34] for a comprehensive summary). REFLEX includes 452 clusters over the southern celestial hemisphere and is more than 90% complete to a flux limit of 3×10^{-12} erg s $^{-1}$ cm $^{-2}$ (in the ROSAT energy band, 0.1-2.4 keV). The volume explored is larger than that of the 2dF survey and comparable to the volume that will be filled by the SDSS 1-million-galaxy redshift survey⁷. The fine structure visible in Fig. 1 is obviously lost in the cluster distribution; however, a number of cluster agglomerates and filamentary structures with large sizes ($\sim 100 h^{-1}$ Mpc) are evident, showing that inhomogeneities are still strong on such very large scales.

4 Statistical Properties of Clustering

4.1 The Power Spectrum of Fluctuations

Large-scale structure models as Λ CDM are specified in terms of a specific shape for the power spectrum of density fluctuations $P(k)$. Analogously to standard signal

in the radio domain, the CMB spectral distortions produced in the direction of a cluster by the Inverse Compton scattering of the CMB photons over the energetic electrons of the intracluster plasma (see e.g. [28] for a review).

⁷ The SDSS will however probe a much larger volume through the luminous-red galaxy sample that will extend to $z \sim 0.5$ [25].

theory, the power spectrum describes the squared modulus of the amplitudes δ_k (at different spatial wavelengths $\lambda = 2\pi/k$) of the Fourier components of the fluctuation field $\delta = \delta\rho/\rho$ [4]. Studying the power spectrum of the distribution of luminous objects on sufficiently large scales, where the growth of clustering is still independent of k , we hope to recover a relatively undistorted information to test the models.

The uncertainties in relating the observed $P(k)$ of, e.g., galaxies to that from the theory are due to (a) nonlinear effects that modify the linear shape below some scale; (b) the unknown relation between the distribution of the light and that of the mass, that is what the models predict. The first problem can be circumvented by pushing redshift surveys to larger and larger scales, as to work well into the linear regime (and/or following nonlinear evolution through numerical simulations). The second one involves knowing the *bias* parameter b .

The bias parameter can be defined either in integral terms, through the ratio between the variances in galaxy counts and in the mass density $b = (\delta n_{gal}(r)/\langle n_{gal} \rangle)_{rms} / (\delta\rho(r)/\langle \rho \rangle)_{rms}$, or differentially as $b^2 = P_{gal}(k)/P_{mass}(k)$. For galaxy surveys, b can only be deduced using additional external constraints on the power spectrum normalization (e.g. from CMB anisotropies, that directly probe fluctuations in the mass [37]), or studying higher-order moments of the distribution [38]. X-ray selected clusters, on the other hand, have a specific advantage in this respect, as their bias factor can be computed directly once the sample selection function is known (e.g. [39]).

The 2dF and REFLEX surveys have produced the best estimates to date of the power spectrum of galaxies and X-ray clusters, respectively. Fig. 3 (left panel) compares these data sets directly, evidencing the remarkable similarity of the shape of $P(k)$ for these two classes. This provides a direct confirmation of the bias scenario, where clusters form at the rare high peaks of the mass density distribution [40] and for this reason display a stronger clustering amplitude. In the same figure I have also plotted the predictions for the mass power spectrum of two models of the CDM family, computed as described in [41]. A model very close to what we defined as the ‘concordance’ model ($\Omega_M \simeq 0.3$, $\Omega_A \simeq 0.7$, $h = 0.7$) provides in general an excellent fit to the 2dF power spectrum, with a bias parameter (i.e. normalization) close to unity⁸. The upper solid curve, on the other hand, is the same model re-normalized as $P_{clus}(k) = b_{clus}^2 P_{CDM}(k)$ where the cluster bias parameter b_{clus} has been computed taking into account the specific mass distribution function of the cluster sample, using a relatively straightforward theory [42,43] (see [44] for more details). It is for these computations that a well-understood mass selection function of our clustering tracers is crucial. The general result (an additional step with respect to galaxies), is that our fiducial low- Ω_M CDM model is capable to match very well **both** the

⁸ In fact, once we fix the primordial spectrum P_o , in a pure CDM Universe the observed shape depends only on Ω_M , not on Ω_A (which on the other hand influences the normalization). In the literature, this is often parameterized through a *shape parameter* $\Gamma = \Omega_M h f(\Omega_b)$, where $f(\Omega_b) \sim 1$ in case of negligible baryon fraction. The ‘concordance’ model, therefore, has $\Gamma \simeq 0.2$.

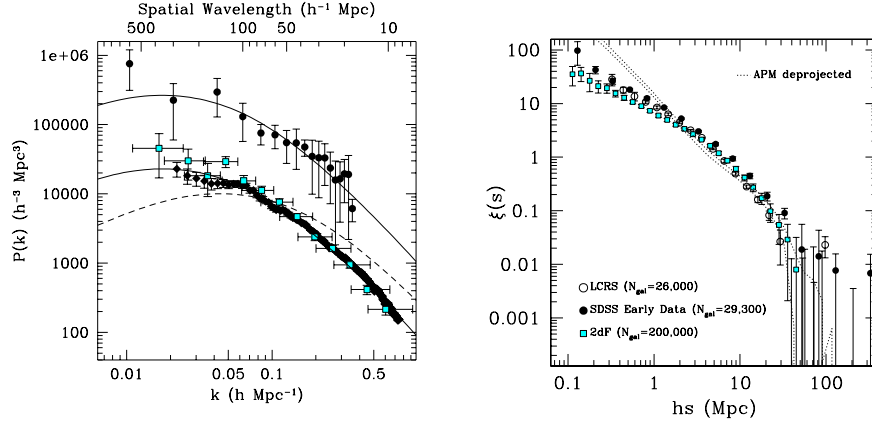


Fig. 3. Left: The power spectrum of 2dF galaxies and REFLEX clusters. *Filled diamonds:* estimate using 147,000 redshifts by the 2dF team [19]; *open squares:* Tegmark et al. [35] thorough analysis of the 100,000-redshift 2dF public release (see Hamilton, this volume); *filled circles:* REFLEX clusters in a $600 h^{-1} \text{ Mpc}$ box [44]. *Dashed line:* Einstein-De Sitter CDM model; *lower solid line:* Lambda-CDM ‘concordance’ model (as defined in the first section); both are normalized to match the amplitude of CMB fluctuations [36]; *upper solid line:* same Lambda-CDM model, but renormalized (“biased”) according to the mass distribution of REFLEX clusters [44,13]. **Right:** The two-point correlation function from the 2dF [55] and SDSS [56] galaxy data, compared to the previous Las Campanas Redshift Survey [57]. The dotted lines show instead a correlation function in *real space*, obtained through deprojection from the APM angular galaxy catalogue [58] under two different assumptions about galaxy clustering evolution.

shape and amplitude of the cluster $P(k)$ [44]. The same shape agrees well also with the power spectrum of the distribution of QSO’s from the 2QZ survey, a large redshift survey of colour-selected quasars carried out using the same 2dF spectrograph at the Anglo-Australian Telescope [45].

As can be seen from fig. 3, the low- Ω_M CDM model predicts a maximum for $P(k)$ around $k = 0.02 h \text{ Mpc}^{-1}$. This turnover in the power spectrum is an imprint of the horizon size at the epoch of matter-radiation equality [5] and marks an “homogeneity scale”, above which (smaller k ’s) the variance drops below the white-noise behaviour. In a pure fractal Universe, for example, $P(k)$ would continue to rise when moving to smaller and smaller k ’s [46]. In fact, at least visually the data of Fig. 3 do not really show a convincing indication for a maximum. In addition, on such extremely large scales ($\lambda > 500 h^{-1} \text{ Mpc}$), the effect of the survey geometry on the measured power can be very significant, resulting in an effective survey *window function* in Fourier space which is convolved with the true underlying spectrum (e.g. [35]). For highly asymmetric geometries, the plane-wave approximation intrinsic in the Fourier decomposition fails, and the convolution with the window function easily mimics a turnover in

a spectrum with whatever shape (e.g [47]). The best solution in such cases is to resort to survey specific eigenfunctions as those provided by the Karhunen-Loeve (KL) transform [48]. This technique has been intensively applied to the REFLEX data [49], confirming a shape corresponding to $\Omega_M \simeq 0.2 - 0.4$ (corresponding to a turnover $k \simeq 0.02 h \text{ Mpc}^{-1}$). A more recent KL analysis using the joint constraints from both the REFLEX mass function and power spectrum, provides a much stronger result, $\Omega_M = 0.34 \pm 0.03$, together with a power spectrum normalization $\sigma_8 = 0.71 \pm 0.04$ (expressed in the conventional form as the variance within $8 h^{-1} \text{ Mpc}$ -radius spheres) [50]. This normalization agrees very well with the completely independent value obtained from a joint analysis of the 2dF survey and CMB data [37].

The SDSS will be the best data set to study the details of the power spectrum around the peak scale. Preliminary results based on a small subset of the survey [51,52] indicate a best-fitting CDM spectral shape $\Gamma = 0.14^{+0.11}_{-0.06}$, i.e. virtually the same as measured by 2dF and REFLEX. Again, we see an impressive convergence of independent observations towards the same low- Ω_M CDM model. The SDSS luminous red-galaxy sample, in particular, will be unique to investigate the presence of *baryonic features* in the power spectrum, produced by oscillations in the baryonic matter component within the last-scattering surface [41,53]. These features are expected to be of very low amplitude unless the baryon density is much higher than currently established and thus require a very high signal-to-noise and frequency resolution in $P(k)$. Potential wiggles seen in the 2dF power spectrum, in fact, are shown to be an artifact of the survey window function and the strong bin-to-bin correlation [19,35].

4.2 The Two-Point Correlation Function

In fact, the simplest statistics one can compute from the data and also that for which the selection function is more directly corrigible, is not the power spectrum, but rather its Fourier transform, the *two-point correlation function* $\xi(r)$, which measures the excess probability over random to find a galaxy at a separation r from a given one [54]. Fig. 3 (right panel) shows the correlation function measured in *redshift space*, $\xi(s)$ (see next section), from the 2dF and SDSS current data sets [55,56], compared to the LCRS [57]. Also shown (dotted lines) is the real-space $\xi(r)$ reconstructed from the APM angular survey [58]. The shape of $\xi(s)$ is roughly a power law $\sim (s/s_o)^{-\gamma}$ between 0.1 and $30 h^{-1} \text{ Mpc}$, with a *correlation length* $s_o \simeq 8 h^{-1} \text{ Mpc}$. The overall difference with the $\xi(r)$ from the APM survey (which is in real space, being based on a deprojection of angular clustering), is due to redshift-space effects, that I will address in detail in the next section. Note how $\xi(s)$ maintains a low-amplitude, positive value out to separations of more than $50 h^{-1} \text{ Mpc}$, with the 2dF and SDSS data possibly implying a zero-crossing scale approaching $100 h^{-1} \text{ Mpc}$. This comparison shows explicitly why large-size galaxy surveys are so important, given the weakness of the clustering signal at such large separations⁹.

⁹ There is quite a bit of confusion in technical papers on the term “scale” when comparing results from power spectra and correlation function analyses. A practical

4.3 Velocity Distortions in the Redshift-Space Pattern

The separation s between two galaxies computed using their observed redshifts is not a true distance: the red-shift observed in the galaxy spectrum is in fact the quantity $cz = cz_{\text{cosmological}} + v_{\text{pec}||}$, where $v_{\text{pec}||}$ is the component of the galaxy peculiar velocity along the line of sight. This contribution is typically of the order of 100 km s^{-1} for galaxies in the general field, but can rise above 1000 km s^{-1} within high-density regions as rich clusters of galaxies. Fig. 3 shows explicitly the consequence of such *redshift-space distortion* for the correlation function: $\xi(s)$ (all points) is *flatter* than its real-space counterpart (dotted lines). This is the result of two concurrent effects: on small scales ($r \lesssim 2 h^{-1} \text{ Mpc}$), clustering is suppressed by high velocities in clusters of galaxies, that spread close pairs along the line of sight producing what in redshift maps are sometimes called “Fingers of God”. Some of these are perhaps recognisable in Fig. 1 as thin radial structures. On the other hand, large-scale coherent streaming flows of galaxies towards high-density structures enhance the apparent contrast of these, when seen perpendicularly to the line of sight. This effect, on the contrary, amplifies $\xi(s)$ above $\sim 3 - 5 h^{-1} \text{ Mpc}$.

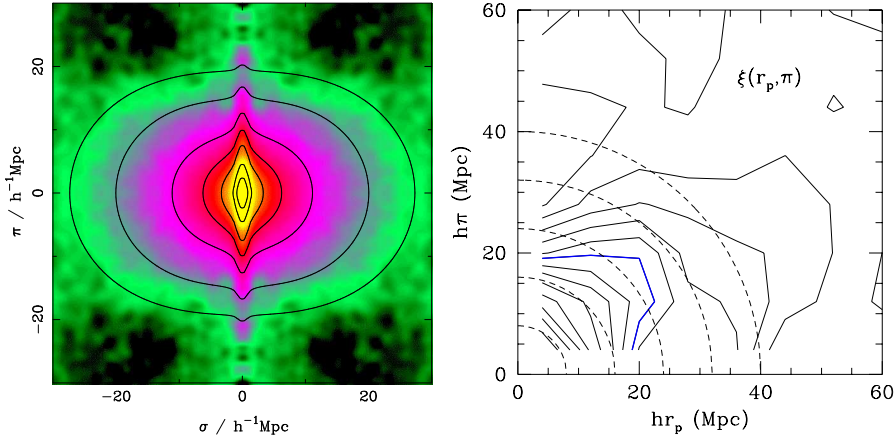


Fig. 4. Left: The bi-dimensional correlation function $\xi(r_p, \pi)$ from the 2dF redshift survey (with r_p named here σ). The large-scale deviation from circular symmetry is a measure of the level of infall of galaxies onto superclusters, proportional to $\beta = \Omega^{0.6}/b \simeq 0.43$ [14]. **Right:** the same, but for the REFLEX survey of X-ray clusters of galaxies (plotting only the first quadrant). Note also here the compression of the contours along the redshift (π) direction, implying significant streaming velocities of clusters towards high-density regions. Note also the lack of any stretching at very small r_p 's (there are no “Fingers of God” made by clusters!) [59,64].

“rule of thumb” which works about right with well-behaved spectra is that a scale k in the power spectrum, corresponding to a spatial wavelength $\lambda = 2\pi/k$, relates approximately to $r \sim \lambda/4$ in $\xi(r)$.

Such peculiar velocity contribution can be disentangled by computing the two-dimensional correlation function $\xi(r_p, \pi)$, where the separation vector s between a pair of galaxies is decomposed into two components, π and r_p , parallel and perpendicular to the line of sight respectively (see [60] for details). The result is a bidimensional map, whose iso-correlation contours look as in Fig. 4, where the 2dF $\xi(r_p, \pi)$ is plotted [14].

Redshift-space distortions contain important information as galaxy motions are a direct dynamical probe of the mass distribution [61]. Non-linear distortions are a measure of the “temperature” of the galaxy soup on small scales, and they are in principle related to Ω_M through a *Cosmic Virial Theorem* [54], which however has been shown to be difficult to apply in practice to real data [62]. Linear distortions produced by infall provide a way to measure the parameter $\beta = \Omega_M^{0.6}/b$, i.e. essentially the mass density of the Universe modulo the bias parameter. As thoroughly explained in the excellent review by Andrew Hamilton [60], this can be achieved by measuring the oblate compression of the contours of $\xi(r_p, \pi)$ along π . One way to do this is to expand $\xi(r_p, \pi)$ in spherical harmonics. In linear perturbation theory, only the monopole $\xi_0(s)$, quadrupole $\xi_2(s)$ and hexadecapole $\xi_4(s)$ are non-zero, and it has been shown [60] that β can in principle be derived directly through a combination of these quantities. In practice, linear and non-linear effects are interlaced out to fairly large scales ($\sim 20 \text{ h}^{-1} \text{ Mpc}$), and require a careful modeling also for a survey as large as the 2dF. This has been done¹⁰ [14], showing that the quadrupole-to-monopole ratio of the map of Fig. 4 requires a Universe with $\beta = 0.43 \pm 0.07$. If 2dF galaxies are unbiased ($b \simeq 1$), this leads to $\Omega_M \simeq 0.25$.

Clusters of galaxies clearly also partake in the overall motion of masses produced by cosmological inhomogeneities. Line-of-sight spurious effects (as projections in optically-selected cluster catalogues [63] or large redshift errors) and limited statistics, prevented so far the detection of true velocity anisotropies in cluster $\xi(r_p, \pi)$ maps. Fig. 4 plots $\xi(r_p, \pi)$ for the REFLEX survey, which shows evidence for the compression of the contours along the line of sight, of the kind expected by the linear infall of clusters towards superstructures [64].

5 Summary

We are definitely in a golden age for observational cosmology and in particular for the study of large-scale structure. We never had such a wealth of diverse data at our disposal, through which we are pinning down the values of cosmological parameters to a high accuracy (e.g. [2]). The observational facts we have reviewed here contribute to further reinforce the remarkable convergence among different observables (CMB, large-scale structure, distant Supernovae, cluster evolution, to mention a few) towards a model with flat geometry ($\Omega_{total} = 1$) provided by the combination of a dominating Cold Dark Matter component ($\Omega_M = \Omega_{CDM} +$

¹⁰ A more careful analysis applied to the 100,000 redshift public release [35], measures essentially the same value of β , but with a 1- σ error of ± 0.16 , as discussed by Hamilton in his contribution to this volume.

$\Omega_{\text{baryon}} \simeq 0.3$, with $\Omega_{\text{baryon}} \simeq 0.04$) and a Dark Energy of unknown nature (the cosmological constant, $\Omega_\Lambda \simeq 0.7$).

Still, we cannot avoid to note that such wonderful “standard” cosmological model is full of “unseen” ingredients, as a dark matter nobody has detected so far (but see contribution by P. Belli in this volume) and a dark energy we have little idea where it could come from. Seen from outside, this might look as an almost epicyclic model and I believe understanding its foundations provides one of the major challenges for particle physics and cosmology in the next decade.

Acknowledgments. I thank the organizers of the DARK2002 meeting for inviting me to give this review. I am grateful to all my collaborators for all our common results discussed here, in particular P. Schuecker, C. Collins and H. Böhringer. I thank I. Zehavi and E. Hawkins for providing their clustering results in electronic form.

References

1. Blumenthal, G.R., et al.: *Nature* **311**, 517 (1984)
2. De Bernardis, P., et al.: *Nature* **404**, 955 (2000)
3. Perlmutter, S., Riess, A.: in “COSMO-98: II Int. Workshop on Particle Physics and the Early Universe”, D.O. Caldwell ed., AIP Conference Proceedings, vol. 478., (Woodbury, NY 1999), p. 129
4. Peacock, J.A.: *Cosmological Physics* (Cambridge University Press, Cambridge 1999)
5. Padmanabhan, T.: *Structure Formation in the Universe* (Cambridge University Press, Cambridge 1993)
6. White, S.D.M., & Rees, M.J.: *MNRAS*, **183**, 341 (1978)
7. Jenkins, A., et al.: *MNRAS* **321**, 372 (2001)
8. Somerville, R.S.: *MNRAS* **320**, 504 (2001)
9. Kauffmann, G., Charlot, S., Haehnelt, M.: *Phil. Trans. of the Royal Soc. of London, Series A, Vol. 358*, p. 2121 (2000)
10. Cole, S., et al.: *MNRAS* **319**, 168 (2000)
11. Silva, L., et al.: *Ap&SS* **276**, 1073 (2001)
12. Maddox, S.J., et al.: *MNRAS* **242**, 43p (1990)
13. Borgani S., Guzzo L.: *Nature* **409**, 39 (2001)
14. Peacock, J.A., et al. (the 2dF Team): *Nature* **410**, 169 (2001)
15. Rood, H.J.: *ARA&A* **26**, 245 (1998)
16. Colless, M., et al. (the 2dFGRS team): *MNRAS* **328**, 1039 (2001)
17. Shectman, S.A., et al.: *ApJ* **470**, 172 (1996)
18. Vettolani, G., et al. (the ESP team): *A&AS*, **130** 323 (1998)
19. Percival, W., et al. (the 2dFGRS team): *MNRAS* **327** 1297 (2001)
20. Peacock, J.A. & the 2dFGRS team: in *20th Texas Symposium on Relativistic Astrophysics*, (Austin, December 2000), in press (2002) (astro-ph/0105450)
21. York, D.G., et al. (the SDSS Collaboration): *AJ*, **120** 1579 (2000)
22. Fernández-Soto, A.: *Ap&SS*, **276**, 965 (2001)
23. Yee, H.: in *Xth Rencontres de Blois: The Birth of Galaxies*, in press (1998) (astro-ph/9809347)
24. Becker, R.H. & the SDSS Collaboration: *AJ*, in press (2002) (astro-ph/0108097)
25. Eisenstein, D.J., et al. (the SDSS Collaboration): *AJ*, **122** 2267 (2001)

26. Guzzo, L.: in *XIXth Texas Symposium on Relativistic Astrophysics & Cosmology*, Nucl. Phys. B (Proc. Suppl.) vol.80, p.233 (09/06), E. Aubourg et al. eds. (2000) (ext. version in astro-ph/9911115)
27. Nichol, R.C.: in *Tracing Cosmic Evolution with Galaxy Clusters*, ASP Conf. Series, S. Borgani et al. eds., in press (2002) (astro-ph/0110231)
28. Bartlett, J.G.: in *Tracing Cosmic Evolution with Galaxy Clusters*, ASP Conf. Series, S. Borgani et al. eds., in press (2002) (astro-ph/0111211)
29. Ellis, R.S.: in *Tracing Cosmic Evolution with Galaxy Clusters*, ASP Conf. Series, S. Borgani et al. eds., in press (2002) (astro-ph/0112540)
30. Borgani, S., et al.: ApJ **561**, 13 (2001)
31. Rosati, P., et al.: ApJ **445**, L11 (1995)
32. Böhringer, H., et al. (the REFLEX Team): A&A **369**, 826 (2001)
33. Henry, J.P.: in “AMiBA 2001: High-z Clusters, Missing Baryons, and CMB Polarization”, in press (2002) (astro-ph/0109498)
34. Rosati, P., Borgani, S., & Norman, C.: ARAA, in press (2002)
35. Tegmark, M., Hamilton, A.J.S., Xu, Y.: MNRAS, in press (2002) (astro-ph/0111575)
36. Bunn, E.F., & White, M.: ApJ **480**, 6 (1997)
37. Lahav, O., et al. (the 2dFGRS team): MNRAS, in press (2002) (astro-ph/0112162)
38. Verde, L., et al. (the 2dFGRS team): MNRAS, in press (2002) (astro-ph/0112161)
39. Moscardini, L., et al.: MNRAS **316**, 283 (2000)
40. Kaiser, N.: ApJ **284**, L9 (1984)
41. Eisenstein, D.J., Hu, P.: ApJ **496**, 605 (1998)
42. Mo, H.J., & White S.D.M.: MNRAS **282**, 347 (1996)
43. Sheth, R.K., Mo, H.J., Tormen, G.: MNRAS **323**, 1 (2001)
44. Schuecker, P., et al. (the REFLEX Team): A&A **368**, 86 (2001)
45. Hoyle, F., et al.: MNRAS **329**, 336 (2002)
46. Guzzo, L.: New Astronomy **2**, 517 (1997)
47. Carretti, E., et al.: MNRAS **324**, 1029 (2001)
48. Vogeley, M.S., Szalay, A.S.: ApJ **465**, 34 (1996)
49. Schuecker, P., Guzzo, L., Böhringer, H., Collins, C.A.: MNRAS, in press (2002a)
50. Schuecker, P., Böhringer, H., Guzzo, L., Collins, C.A.: in preparation (2002b)
51. Szalay, A.S., et al. (the SDSS Collaboration): ApJ, submitted (2001) (astro-ph/0107419)
52. Dodelson, S., et al. (the SDSS Collaboration): ApJ, submitted (2001) (astro-ph/0107421)
53. Miller, C.J., Nichol, R.C., Batuski, D.J.: ApJ **555**, 68 (2001)
54. Peebles, P.J.E.: *The Large-Scale Structure of the Universe*, (Princeton University Press, Princeton 1980)
55. Hawkins, E., et al. (the 2dFGRS team): in preparation (2002)
56. Zehavi, I., et al. (the SDSS Collaboration): ApJ **571**, in press (2002) (astro-ph/0106476)
57. Tucker, D.L., et al.: MNRAS **285**, L5 (1997)
58. Baugh, C.M.: MNRAS **280**, 267 (1996)
59. Collins, C.A., et al. (the REFLEX Team): MNRAS **319**, 939 (2000)
60. Hamilton, A.J.S.: in *The Evolving Universe. Selected Topics on Large-Scale Structure and on the Properties of Galaxies*, (Kluwer, Dordrecht 1998), ASSL Series, vol. 231, p. 185 (also, astro-ph/9708102).
61. Kaiser, N.: MNRAS **227**, 1 (1987)
62. Fisher, K.B., et al.: MNRAS **267**, 927 (1994)
63. Collins, C.A., et al.: MNRAS **274**, 1071 (1995)
64. Guzzo, L. et al. (the REFLEX Team): in preparation (2002)